2024 International Nuclear Atlantic Conference – INAC 2024
Escola de Guerra Naval, Rio de Janeiro, RJ, May 6 - 10, 2024

ISBN: 978-65-594-1256-3

Analysis of the Impact of Digital Image Format on the Evaluation of a Mammography Phantom

L.F.M. Almeida[1], R.F. Silva[1,2], C. Engler[1], E.R. Leite[1], P. L. Squair[1], M.S. Nogueira[1] and F.G. Guimarães[2]

[1] *laila.almeida@cdtn.br; roger.silva@cdtn.br; camila.engler@cdtn.br; elaine.leite@cdtn.br; peterson.squair@cdtn.br; mnogue@cdtn.br, Centro de Desenvolvimento da Tecnologia Nuclear (CDTN/CNEN) Postal code 31270-901, Belo Horizonte, MG, Brazil*

[2] *roger.silva@cdtn.br; fredericoguimaraes@ufmg.br, Programa de Pós-Graduação em Engenharia Elétrica - Universidade Federal de Minas Gerais - Av. Antônio Carlos 6627, 31270-901, Belo Horizonte, MG, Brazil*

1. Introduction

Since the introduction of digital mammography systems, image files have adopted the DICOM (Digital Imaging and Communications in Medicine) format as the standard for reporting, storage, and transfer, due to its integration with communication systems and medical equipment. The DICOM format, which includes a header and sets of image data, allows these to be compressed into a single file and also enables adjustments to the image contrast window, in addition to offering high resolution [1]. However, the files are bulky, making storage and transmission difficult, and they are not recognized by common Windows® software, requiring additional software. Therefore, it is crucial to explore different formats to assist in interpretation and transmission between equipment and specialists [1,2]. In this context, this study aims to visually and objectively assess the quality of digital mammography phantom images using different file formats (DICOM, JPG at four quality levels: 85, 90, 95, and 100% (8 bits), and PNG with lossless compression (8 bits)), as well as quantify the influence of compressions in each image format.

2. Methodology

For the study, the accreditation phantom from the American College of Radiology (ACR), as presented in Figure 1, was utilized. This phantom contains internal objects that simulate structures found in a breast [3,4]. Image acquisition was performed using a mammography image receptor of the Retrofit DR type, manufactured by iRay, with dimensions of 24x30 cm, attached to an analog mammography unit. Image conversion to different file formats was conducted using the Python programming language. Visual analysis was carried out on a high-resolution Planar monitor, model X: 0.285, Y: 0.307, LCD 5MP, and objective parameters were measured using the free software ImageJ [5].

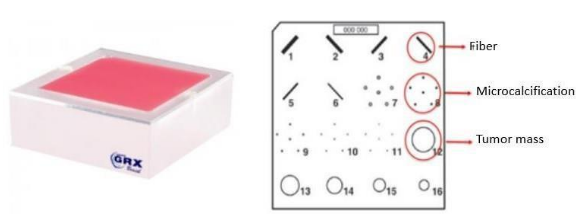

Figure 1: Presentation of the phantom ACR and their respective analysis structures.

The image acquisition was performed by standardizing the voltage at 28 kVp and varying the mAs (20, 40, 50, 56, 63, 71, 80, 90, 100), as well as the target-filter combination (Molybdenum-Molybdenum (MoMo), Molybdenum-Rhodium (MoRh), and Tungsten-Rhodium (WRh)). Subsequently, the images were normalized and converted to 8-bit formats using the Python programming language, resulting in a sample containing 162 images. These images were then exported to the diagnostic monitor, where they were visually evaluated for structures such as fibers, microcalcification, and tumor masses [3]. For objective analysis, the Signal-to-Noise Ratio (SNR) metric was used, which can be calculated by the mean pixel value (MPV) of the background divided by the standard deviation (SD) of the background, as demonstrated in Equation 1 [2,6].

$$SNR = \frac{MVP_{BG}}{SD_{BG}} \tag{1}$$

For objective analysis, a 12x12 mm [2,7] Region of Interest (ROI) was defined at the center of the simulator, selecting an area with relative homogeneity and without overlapping structures, as illustrated in Figure 2. From this ROI, MPV and SD values were extracted, which were then used to perform the necessary calculations in Excel® software. The data was then statistically analyzed and represented in bar and scatter plots. To process the objective data, initially, the SNR values for the DICOM format were plotted for all target-filter combinations and parameters used as a reference. Next, the differences between the SNR values of the DICOM format and the other formats were calculated, as were the relative differences obtained by dividing the differences by the SNR of the DICOM format. The subjective data were statistically analyzed using the paired T-test and represented in bar graphs.

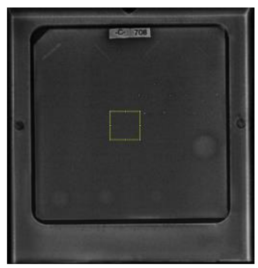

Figure 2: Demonstration of the phantom ACR and their respective ROI.

To analyze the objective data, initially, the SNR values for the DICOM standard were plotted for all target-filter combinations and parameters used, to serve as a reference. Next, the differences between the SNR values of the DICOM format and the other formats were calculated. Additionally, the relative difference was obtained by dividing the previously obtained difference by the SNR of the DICOM standard. The subjective data were statistically analyzed using the paired T-test and represented in bar graphs.

3. Results and Discussion

Figure 3 shows the SNRs obtained for DICOM images at different exposure parameters, from which it can be inferred that for all target-filter combinations, the SNR tends to decrease. This is due to the progressively increasing applied load, which consequently darkens and reduces the SNR. Additionally, the best filter for a compressed phantom of 4.5 cm is MoMo, which exhibits greater stability and a real trend, except for one outlier point at 56 mAs.

Figures 4 (a, b, and c) illustrate the relative difference between the image formats compared to the DICOM standard. The greater the relative difference, the farther the results are from the DICOM standard and, consequently, the greater the difference in image quality compared to DICOM. Thus, the figures respectively depict the results for the MoMo, MoRh, and WRh combinations. The formats with the poorest results were those at the extremes (JPG Q85 and JPG Q95), while the JPG Q100 format performed better, varying within 0%. The relative differences varied little, around 2% for all formats (except JPG Q85), indicating that SNR is not the appropriate metric to show significant variations in processed images. Further studies should be conducted using raw data images (without processing).

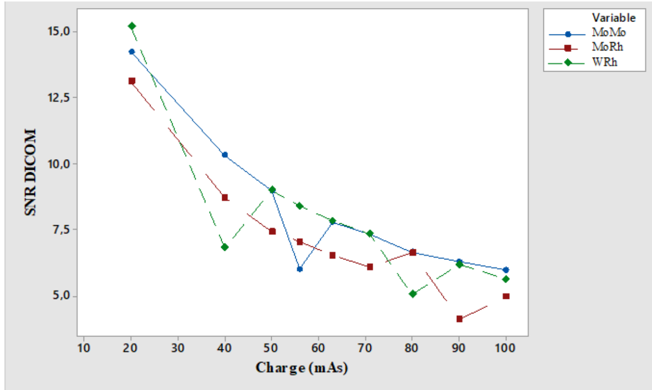

Figure 3: Scatter plot of the SNR for DICOM images.

(a) (b) (c)

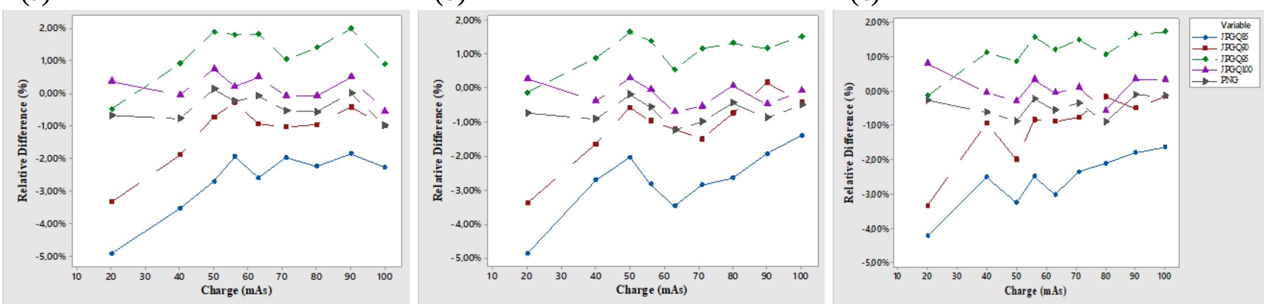

Figure 4: Scatter plots illustrating the SNR metric for the different formats and parameters in the following target - filter combinations: (a) MoMo; (b) MoRh; and (c) WRh.

Figure 5 illustrates the discrepancies in means observed among image formats for phantom structures. Thus, the greater this difference, the farther from the DICOM standard the format will be and the poorer its performance will be. The format that showed the greatest discrepancy was JPG Q85 for all structures, while PNG had the smallest discrepancy for microcalcification and masses, possibly due to its lossless compression process. It is important to note that the JPG Q100 format yielded satisfactory results for fibers and tumor masses, as well as in the SNR metric; however, its performance was inferior for microcalcification. This can be explained by the lack of utilization of an objective metric that evaluates high-contrast structures, such as the contrast-to-noise ratio (CNR).

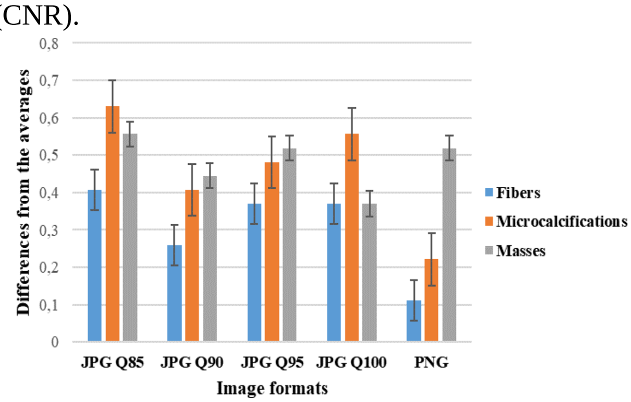

Figure 5: A stacked bar graph illustrating the differences in structure averages for the different formats for the ACR phantom.

4. Conclusions

It is concluded that the format of digital images significantly impacts the image quality of the ACR phantom. It was observed that the JPG Q100 format yielded more favorable results, with smaller differences compared to the DICOM standard. Conversely, the JPG Q85 and JPG Q95 formats performed the worst, indicating a greater difference in image quality. In the visual analysis, PNG was the only format not to show statistically significant differences in fibers and microcalcification compared to DICOM images, suggesting similar or close image quality. Additionally, the observed difference in the averages of phantom structures highlighted the superiority of the PNG format in maintaining fidelity to structures, while JPG Q85 exhibited the greatest discrepancy compared to the DICOM standard. It is important to note that although the PNG format does not undergo losses in the compression process and theoretically should obtain results equal to DICOM, the subsequent decrease in image quality and contrast resolution in this study was due to the reduction of bit depth from 14 to 8 in the conversion process.

It is necessary to highlight that, overall, all formats are within the acceptable response range. These findings underscore the importance of considering the digital image format in evaluating the image quality of a mammography phantom, especially when selecting the most appropriate format to ensure an accurate representation of anatomical structures. It is recommended that future studies conduct a more in-depth analysis of image quality, utilizing other objective metrics, varying observers, and using other types of mammography phantoms.

Acknowledgements

This work was supported by the Brazilian National Council for Scientific and Technological Development (CNPq, INCT/INAIS Project – 406303/2022-3 and CNPq Process 308368/2022-3 – Productivity Fellowship), the Minas Gerais State Research Support Foundation (FAPEMIG), the Nuclear Technology Development Center (CDTN), and the Federal University of Minas Gerais (UFMG).

References

[1] R.V. Dandu. Managing DICOM images: Tips and tricks for the radiologist. *Indian J Radiol Imaging.* Jan;22(1):4-13. doi: 10.4103/0971-3026.95396. PMID: 22623808; PMCID: PMC3354356 (2012).

[2] M.V., Murilo et al. DICOM file format has better radiographic image quality than other file formats: an objective study. *Brazilian Dental Journal*, v. 34, p. 150-157, (2023).

[3] ANVISA. Ministério da Saúde (BR), Agência Nacional de Vigilância Sanitária, Diretoria Colegiada. Instrução normativa - IN no 92, de 27 de maio de 2021. Dispõe sobre requisitos sanitários para a garantia da qualidade e da segurança de sistemas de mamografia, e dá outras providências. Diário Oficial da União, Brasil (in Portuguese) (2022).

[4] SILVA, F. A. R.; VIEIRA, L. A. Programa Estadual de Controle de Qualidade em Mamografia – PECQMamo: Instrutivo do Programa Estadual de Controle de Qualidade em Mamografia. Disponível em: < http://atalanta.cdtn.br/>. Acesso em: 10 de março de 2023 (in Portuguese) (2017).

[5] WIDE. https://wide-usa.com/?gad_source=1&gclid=Cj0KCQiA2eKtBhDcARIsAEGTG43sieE_9lrX4Z7oJP9DruMMoYhpnZKs5PZyyh9QZH1VIn7es8df9rsaAoFoEALw_wcB (2024).

[6] IAEA. INTERNATIONAL ATOMIC ENERGY AGENCY. Human health series N17.: Quality Assurance Program for Digital Mammography, 1 ed. Vienna, 2011. 195p (2011).

[7] SOC. ESPANHOLA DE FÍSICA MÉDICA. SOC. ESPANHOLA DE PROTEÇÃO RADIOLÓGICA. SOC. ESPANHOLA DE RADIOLOGIA MÉDICA. Protocolo Espanhol de Controle de Qualidade em Radiodiagnóstico. Editora Senda S.A. Revisão 2011 (in Portuguese) (2011).